# Energy and Spectrally Efficient Signalling for Next Generation IoT

Xinyue Liu and Izzat Darwazeh
Dept. of Electronic and Electrical Engineering
University College London
London WC1E 7JE, UK
{x.liu.17, i.darwazeh}@ucl.ac.uk

*Abstract*—This work proposes an energy and spectrally efficient signalling technique for the next generation internet of things (IoT). The signalling method employs the bandwidth compressed fast-orthogonal frequency division multiplexing (FOFDM) scheme with the single dimensional pulse amplitude modulation (PAM) as well as the frequency orthogonal filtering technique using Hilbert transform (HT) pair. The proposed HT-FOFDM system is designed and modelled based on the narrowband IoT (NB-IoT) specifications. To investigate the designed signalling method of different spectral efficiencies, we conducted simulations for HT-FOFDM with comparisons to single-carrier frequency division multiple access (SC-FDMA). We show that the proposed PAM modulated HT-FOFDM signalling increases the data rate effectively while maintaining reliable transmission within the same bandwidth of 180kHz. Comparative results of the bit error rate (BER) performance in additive white Gaussian noise (AWGN) channel and constellation diagrams of received noisy signals are presented. Furthermore, we show that HT-FOFDM with PAM modulation schemes comprehensively outperforms SC-FDMA that achieves the same spectral efficiencies with significant power advantages.

*Index Terms*—next generation IoT, spectral efficiency, energy efficiency, fast-OFDM, Hilbert transform pair

## I. INTRODUCTION

The internet of things (IoT) and 5G wireless technologies are evolving towards the next-generation IoT, assembling technologies such as edge computing, artificial intelligence (AI) and distributed ledger technologies (DLT) and integrating augmented and virtual reality (AR/VR) based services and applications [1]. To support demanding high bit rate applications and ubiquitous connectivity, from the physical layer aspect, new techniques with low complexity, high power efficiency, and increased capacity are necessarily needed.

In five years from now, by 2027, the number of IoT connections is forecast to exceed 30 billion worldwide, and with over half of these are envisioned to be cellular IoT connections [2]. One of the cellular IoT connections standardised in 4G LTE [3], i.e., narrowband IoT (NB-IoT), continues to form part of the 5G standards and therefore coexist with the other 5G new radio (NR) components in the same networks. This indicates a high share of NB-IoT and 5G devices and hence, sets the demand for technologies that support the low power wide area (LPWA) communications in the 5G context. In the case of LPWA, narrowband signalling is adopted to have higher robustness to the severe pass loss in large-scale

transmission. More specifically, NB-IoT employs orthogonal frequency division multiple access (OFDMA) for the downlink transmission and single-carrier frequency division multiple access (SC-FDMA) for its uplink, where a narrowband of 180 kHz is occupied by 12 modulated subcarriers. Due to the ever increasing demand for higher capacity and energy efficiency for ultra-massive connectivity and traffic, there have been much research and several proposals on evolving the physical layer design of IoT, by replacing the orthogonal frequency division multiplexing (OFDM) signalling with more spectrally efficient techniques.

Fast-OFDM (FOFDM) is a variation of OFDM achieving a doubled spectral efficiency [4]. Due to its advantage of doubling the data rate within the bandwidth-limited spectrum while maintaining the transmission reliability, FOFDM has increasingly attracted researchers' interest, consequently leading to a wide application in wireless [5] and optical communications [6], particularly arising rapidly in visible light communications (VLC) in recent years [7] for both single-input single-output (SISO) and multiple-input multiple-output (MIMO) transmissions. FOFDM requires one-dimensional (1D) modulation, which constrains its improvement of spectral efficiency relative to two dimensional schemes, nevertheless, makes it a good fit for IoT standardised systems. In particular, the feasibility of FOFDM for NB-IoT applications has been theoretically investigated and experimentally verified in [8], where FOFDM is shown to an enhanced capacity by $200\%$. Moreover, for the use cases of NB-IoT, FOFDM was combined with index modulation (IM) [9] and filtering technique with Hilbert transform (HT) pair [10], showing the advantages of enhanced power efficiency and quadrupled data rate relative to conventional IoT systems, respectively.

Inspired by the aforementioned work and considering the main demands of next generation IoT integrated with 5G scenarios, this work proposes an energy and spectrally efficient signalling method. Specifically, we employ FOFDM with singular dimensional modulation pulse amplitude modulation (PAM) scheme and the filtering technique with a HT pair [11].

In this paper, we expand on the design in [10] by developing the use of 1D constellation and demonstrating the advantages of using HT-FOFDM in IoT scenarios. Considering the limitation of the maximum achievable spectral efficiency of binary phase shift keying (BPSK), we propose the new

design by utilising the singular dimensional constellation of PAM modulation to maintain the orthogonality in FOFDM signal. Performance comparison of the proposed signals is investigated relative to the QAM modulated SC-FDMA signal under fixed spectral efficiencies. Numerical results show that HT-FOFDM with PAM schemes achieve increased spectral efficiency without degrading the bit error rate (BER) performance. Besides, The HT-FOFDM with PAM outperforms SC-FDMA in terms of less required power when achieving the same data rate and similar error performance at the expense of a limited increase in complexity.

The outline of this paper is as follows; section II briefly discusses the next generation IoT scenarios and describes the design principles of a doubly orthogonal modulation scheme. In section III, we detail the proposed system model and evaluate the system performance with respect to spectral efficiency and error rate performance; finally, section V draws the conclusion.

## II. PROPOSED SIGNALLING DESIGN

### A. Next generation Internet of Things

The next generation IoT, which requires high data rate, is being considered in beyond 5G systems and the envisioned sixth-generation (6G) networks. As the deployment density of IoT devices grows rapidly with the exponentially increasing demands of communications and traffic, from heterogeneous networks and services, the requirements for the key performance indicators such as the spectral efficiency, energy efficiency, reliability and latency are expected to be challenges in the next generation IoT era.

In the current 4G standards, NB-IoT has a channel bandwidth of 200 kHz while data occupies 180 kHz, which is equivalent to one LTE resource block. As discussed previously, OFDMA is employed for downlink while SC-FDMA is used for the uplink transmission mainly due to its RELATIVELY low peak-to-average power ratio (PAPR). $\pi/2$-BPSK and quadrature phase shift keying (QPSK) are mainly used as modulation schemes for NB-IoT. Fig. 1 provides the uplink resource block map for NB-IoT. It is worth noting that, the demodulation reference signals (DM-RS), which is the fourth symbol in each time slot, are intended for channel estimation. In this work, we assume a flat channel and hence, no symbols are adopted as pilot tones in each subframe. In this work, we investigate the new signalling format that follows the NB-IoT specifications, which is detailed in the next sections.

### B. Design Principles: Doubly Orthogonal Modulation Scheme

The orthogonal FOFDM allows doubling of the bit rate relative to OFDM whilst maintaining orthogonality and, therefore, error rate behaviour. This is true when the two systems use the same 1D modulation scheme. The addition of another layer of orthogonality, using HT pair, as in our recent work in [11], would result in a doubly orthogonal system advantageously improving the bit rate by 400%.

The idea of FOFDM was first proposed in [4] by Rodriguez and Darwazeh in 2002 and a similar system termed M-ary
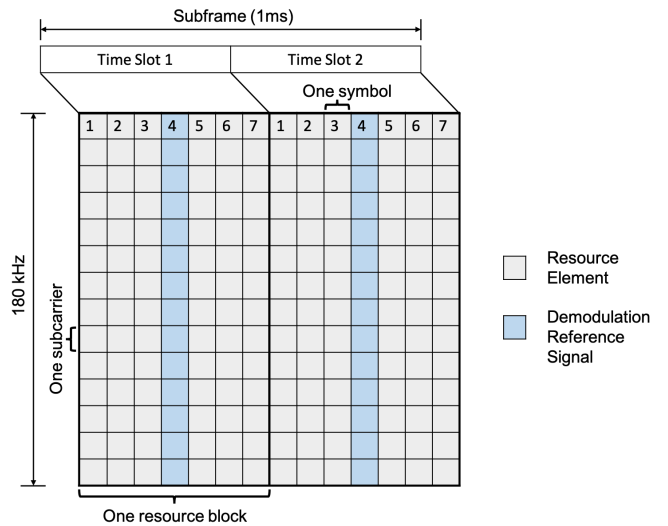


Fig. 1. Uplink resource block definition for NB-IoT. There are 12 subcarriers for 180 kHz bandwidth and 7 symbols bundled into one time slot.

amplitude shift keying (M-ASK) OFDM [12] was developed theoretically in 2003. The attractive feature of FOFDM is that for a given bandwidth-limited spectrum, the FOFDM symbols carry twice the data rate of OFDM when the two systems use the same one-dimensional modulation scheme. The improved data rate is achieved by reducing the multicarrier symbol duration $\mathrm{T_{FOFDM} = T_{OFDM}/2}$ while the subcarrier spacing $\Delta\mathrm{f} = 1/\mathrm{T_{OFDM}}$ remains the same. The normalised FOFDM symbol in the $k^{th}$ signalling interval is given by [4]

$$x(t) = \frac{1}{\sqrt{T}} \sum_{k=-\infty}^{+\infty} \sum_{n=0}^{N-1} X_{n,k} e^{\dfrac{j2\pi nt}{T}}, \quad t \in [0,T], \quad (1)$$

where $N$ is the total number of the subcarriers, $n \in [0, N-1]$ denotes the frequency index of the subcarrier, $X_{n,k}$ represents the symbol transmitted on the $n^{th}$ subcarrier, which is denoted by the exponential component (i.e. $e^{j2\pi nt/2T}$).

The expanded bandwidth frequency separation of FOFDM results in the loss of the orthogonality of the conventional OFDM, constraining its multiplexing/demultiplexing implementation, where the standard discrete Fourier transform (DFT) and its inverse operation are not feasible. To tackle the problem, one of the solutions is to use discrete cosine transform (DCT). Basically, the fast cosine transform (FCT) algorithm is used to perform DCT, where cosine functions with different frequencies are used to express the real-valued subcarriers. In this case, only 1D modulation schemes such as BPSK, M-ASK and PAM can be adopted. The partial symmetry property of inverse fast Fourier transform (IFFT) output of the real-valued input provides another method to implement FOFDM by using the efficient IFFT/FFT operations [13]. The truncation of the IFFT output gives the FOFDM symbols and for the recovery, the conjugations of FOFDM symbols are generated to mend the discarded half of the input
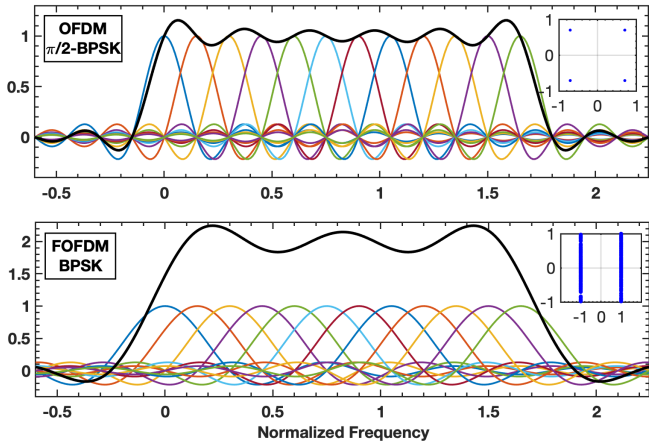
Fig. 2. OFDM and FOFDM subcarriers representations (N = 12) with identical spectrum occupancy while FOFDM provides twice the data rate of OFDM



Fig. 3. BTN pulse and Hilbert filters generated by BTN pulse in time domain

for FFT. In this work, we employ the IFFT/FFT based structure to perform the FOFDM modulation.

Fig. 2 shows the subcarrier representations of OFDM and FOFDM symbols that occupy an identical bandwidth. It can be seen that each FOFDM subcarrier has twice the bandwidth as OFDM while the frequency separations are the same for both sets of 12 subcarriers. Unlike OFDM, the FOFDM subcarriers are only orthogonal when we adopt 1D modulation schemes. In this case, only the in-phase component of the subcarriers carries the data. Considering two arbitrary FOFDM subcarriers, the $e^{j2\pi mt/2T}$ and $e^{j2\pi nt/2T}$ (i.e., the $m^{th}$ and the $n^{th}$ subcarriers) modulated by 1D symbols, the correlation between them that indicates the inter-carrier interference (ICI) is given by:

$$\begin{aligned}
corr(m,n) &= \frac{1}{T}\int_0^T e^{j2\pi mt/2T}e^{j2\pi nt/2T} \\
&= \text{sinc(m - n)} \\
&\quad + j\sin(\frac{\pi(m-n)}{2})\text{sinc}(\frac{(m-n)}{2}),
\end{aligned}$$ (2)

where $T$ represents the FOFDM symbol duration as stated in equation (1). Consequently, the real and imaginary parts of the correlation are

$$\begin{aligned}
\Re\{corr\} &= \text{sinc(m - n)}, \\
\Im\{corr\} &= \sin(\frac{\pi(m-n)}{2})\text{sinc}(\frac{(m-n)}{2}),
\end{aligned}$$ (3)

where $\Re$ and $\Im$ denote the real and imaginary components of a complex expression and the sinc function is defined as $sinc(x) = sin(\pi x)/x$. For the real component $\Re\{corr\}$, the cross-correlations for all $m \neq n$ are zero. This means by transmitting data only via the in-phase dimension of the FOFDM subcarriers, the non-zero cross-correlation of the $\Im\{corr\}$ can be ignored. Therefore, no ICI is introduced to FOFDM when 1D modulation scheme is utilised and the orthogonality remains among the subcarriers.
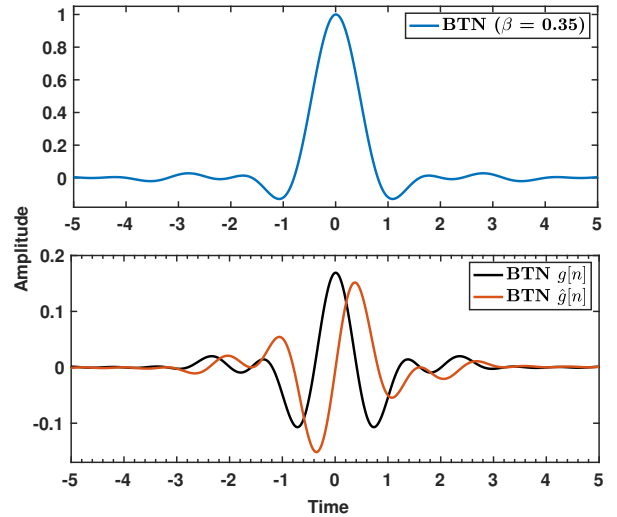
The other layer of orthogonality is introduced by using a filtering technique with HT pair. The orthogonal filter pair is defined by the in-phase (I) and quadrature (Q) component of the discrete analytic signal $g_+[n]$, which is expressed as [14]:

$$g_+[n] = g[n] + j * \hat{g}[n].$$ (4)

In this case, the I component $g[n]$ and Q component $\hat{g}[n]$ are a HT pair. It is worth noting that $\hat{g}[n]$ is the Hilbert transform of $g[n]$ and therefore, the cross-correlation of the pair $\langle g[n], \hat{g}[n]\rangle = 0$, where $\langle \cdot, \cdot \rangle$ denotes an inner product.

The HT pair can be achieved by the product of a basis function $p(t)$ and an orthogonal pair. In this work, we adopt the orthonormal sinusoidal and cosinusoidal signals to generate the HT filter pair, which can be described by:

$$\begin{aligned}
g[n] &= p[n]\cos(\frac{2\pi f_c n}{f_s}), \\
\hat{g}[n] &= p[n]\sin(\frac{2\pi f_c n}{f_s}),
\end{aligned}$$ (5)

where $f_c$ is the carrier frequency and $f_s$ is the sampling rate.

## III. SYSTEM PERFORMANCE ASSESSMENT

### A. System Model

The HT-FOFDM system is illustrated via the block diagram in Fig. 4. At the transmitter, a binary data stream $\mathbf{b} \in \{\mathbf{0}, \mathbf{1}\}$ is generated and mapped into symbols from the PAM-M symbol alphabet, where $M = 2^k$ and k = 1, 2, 3 bits/symbol are for the case of PAM-2, -4 and -8 sequentially that are studied in this work. The PAM-M symbols are divided into two parallel streams equally by the data splitter. Each substream is modulated by 12 FOFDM subcarriers, where the frequency separation between adjacent subcarriers is set to 15 kHz so as to give the overall bandwidth of 180 kHz. It is worth noting that, the modulation processes are independent for the two substreams, though, the same set of FOFDM subcarriers is
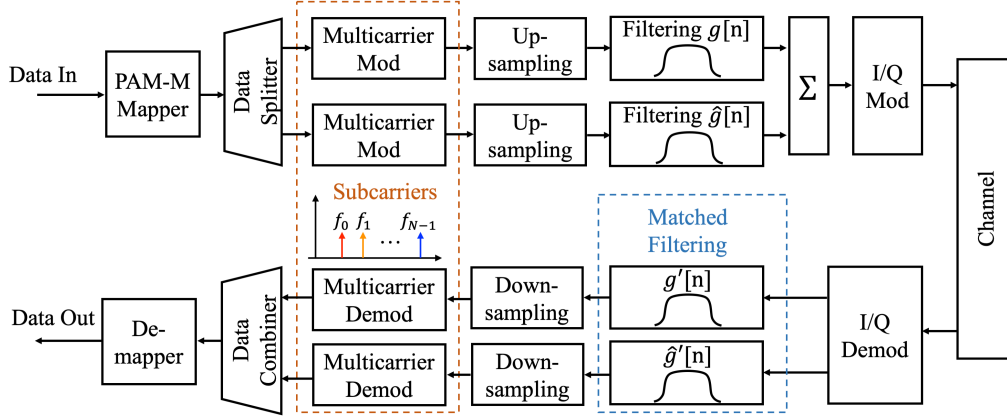
Fig. 4. Block diagram of multicarrier signalling system using Hilbert transform filter pair

employed. After the multicarrier modulation, symbols on both paths are then upsampled by the factor of $q = 4$ via zero-padding between successive samples.

Thereafter, the HT filter pair $g[n]$ and $\hat{g}[n]$ are applied to filter the upsampled symbols. In this work, the HT pair is generated by the basis function with a length of $L = 10$ and roll-off factor $\beta = 0.35$. The parameters are chosen based on investigations in [15] as well as to maintain consistency with the work in [10]. We employ better-than-Nyquist pulse [16], one of the Nyquist pulse family that satisfies the first Nyquist criterion for zero inter-symbol interference (ISI), due to its low out-of-band emission (OOB). The continuous form of the BTN pulse can be given by [16]:

$$p(t) = \frac{\sin[\frac{\pi t}{T_s}][\frac{2\pi\beta t}{T_s \ln(2)}\sin(\frac{\pi\beta t}{T_s} + 2\cos(\frac{\pi\beta t}{T_s}) - 1)]}{(\frac{\pi t}{T_s})[(\frac{\pi\beta t}{T_s \ln(2)})^2 + 1]}, \quad (6)$$

where $T_s$ is the pulse duration. Fig. 3 illustrates the BTN pulse and the corresponding HT pair. After filtering, the two streams of output symbols are summed up for the preparation for I/Q modulation and then passed through the channel. Due to the narrowband property of signalling for IoT scenarios, in this work, we assume the channel is static and the frequency response is almost flat. Therefore, the additive white Gaussian noise (AWGN) channel is used as the channel model.

At the receiver side, the received signals are first processed by the I/Q demodulator. Then the time inverse matched filter pair $g'[n] = g[-n]$ and $\hat{g}'[n] = \hat{g}[-n]$ are used to recover and separate the symbols back into the two substreams. The symbols on the two paths are then downsampled and demodulated by the same set of FOFDM subcarriers. The serial output symbols, given by the data combiner, are demapped into the binary data stream.

### B. Spectral Efficiency and Error Performance

In this section, we evaluate the performance of the proposed PAM modulated HT-FOFDM signal in terms of their spectral
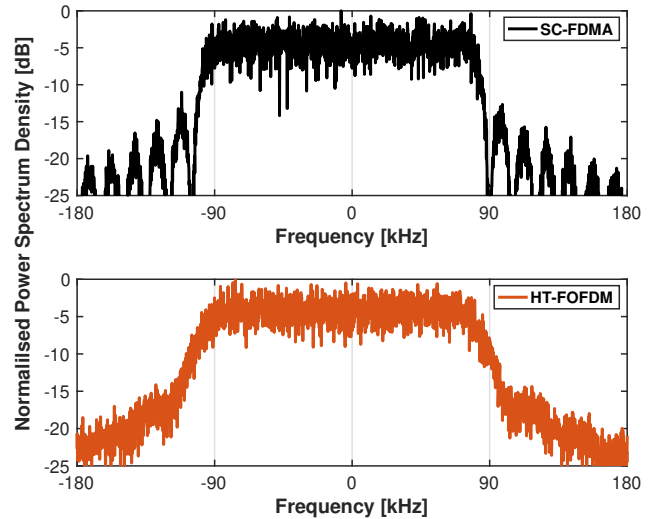


Fig. 5. Spectrum for HT-FOFDM signal occupying the same bandwidth while transmitting at multiple times data rate of SC-FDMA

efficiency and BER performance. For comparison, SC-FDMA is used with QAM schemes considered to obtain the same spectral efficiencies of HT-FOFDM. To show the advantages of HT-FOFDM with 1D PAM modulation, three different schemes, i.e., PAM-2, -4, and -8, are studied to give the spectral efficiency $\eta$ of 4, 8 and 12 bits/s/Hz.

The power spectra of SC-FDMA and HT-FOFDM signals are shown in Fig. 5, where 12 subcarriers are modulated by $\pi/2$-BPSK for SC-FDMA and PAM-2 for HT-FOFDM ($M = 2$). It is worth noting that both signals occupy the same bandwidth of 180 kHz while the HT-FOFDM achieves quadrupled spectral efficiency compared to SC-FDMA.

Two comparisons of BER results are presented in Fig. 7 and Fig. 8 to show the power advantages of HT-FOFDM over the conventional signalling for IoT uplink transmission. Fig.
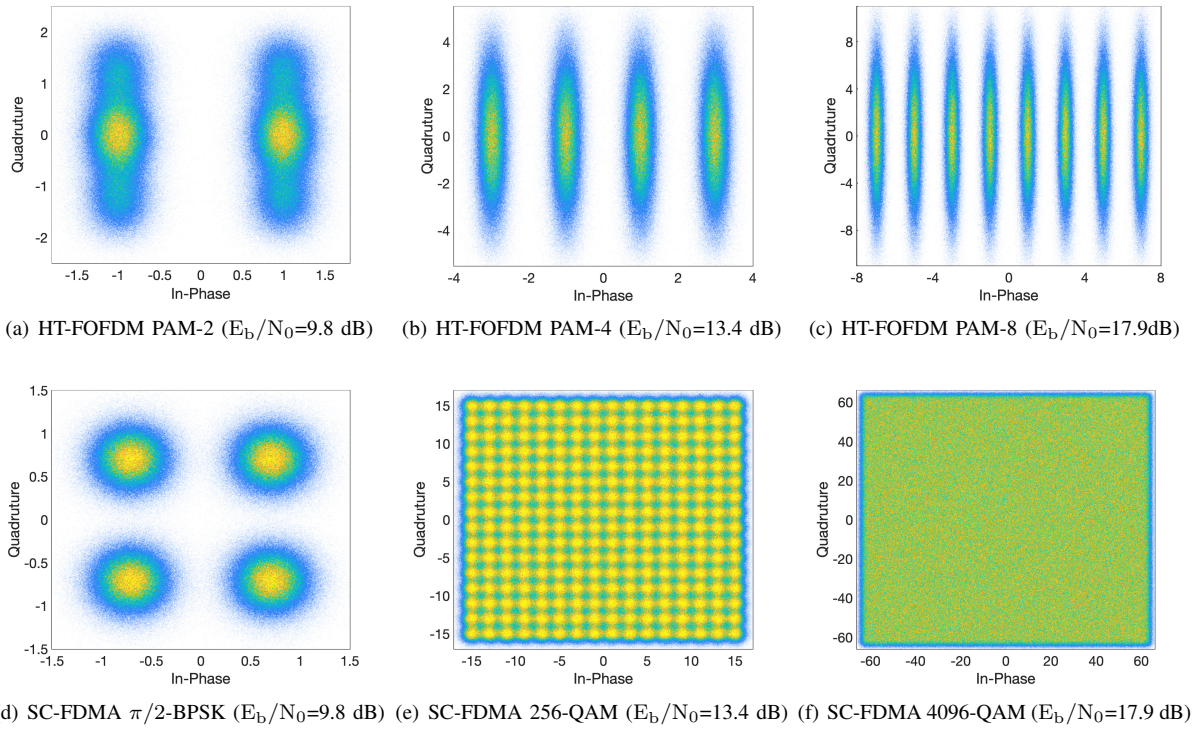
(a) HT-FOFDM PAM-2 ($E_b/N_0$=9.8 dB)    (b) HT-FOFDM PAM-4 ($E_b/N_0$=13.4 dB)    (c) HT-FOFDM PAM-8 ($E_b/N_0$=17.9dB)



(d) SC-FDMA $\pi/2$-BPSK ($E_b/N_0$=9.8 dB)    (e) SC-FDMA 256-QAM ($E_b/N_0$=13.4 dB)    (f) SC-FDMA 4096-QAM ($E_b/N_0$=17.9 dB)

Fig. 6.   Constellation Diagrams of received noisy HT-FOFDM and SC-FDMA signals at varying $E_b/N_0$
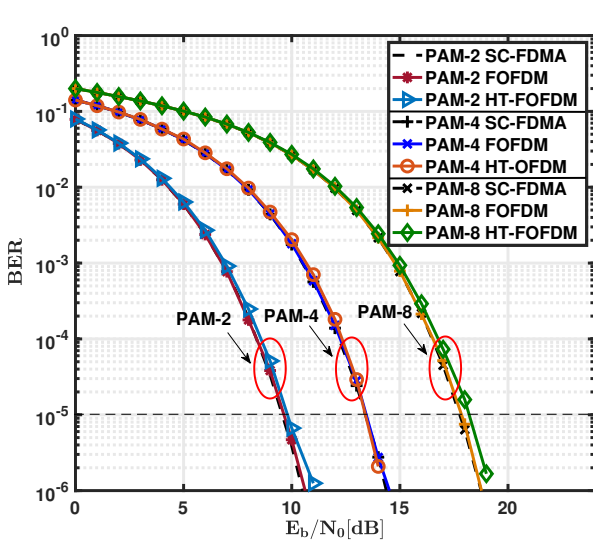


Fig. 7.   BER performance comparison for SC-FDMA, FOFDM and HT-FOFDM with varying order of PAM modulations
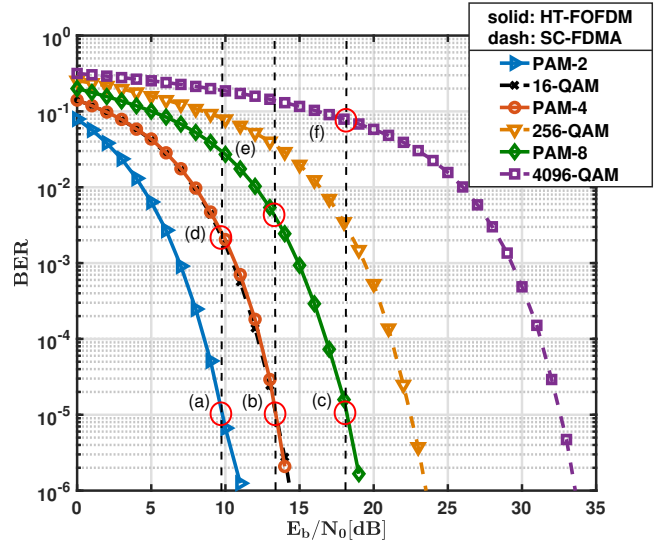


Fig. 8.   BER performance comparison for PAM-M HT-FOFDM and SC-FDMA with high-order QAM modulations that achieve the same spectral efficiency

7 compares the BER performance of proposed HT-FOFDM signalling based on the system given in Fig. 4. The energy per bit to noise ratio $E_b/N_0$ in dB is used for the signal-to-noise ratio (SNR) for performance assessment in the study. The comparison is held for three different levels of PAM modulations ($M$ =2, 4, 8) and three different schemes, i.e., HT-FOFDM, FOFDM and SC-FDMA. It can be seen that the

combined use of waveform compressed FOFDM and HT filter pair improves the data rate without degrading the BER performance. Fig. 8 depicts that the proposed HT-FOFDM with 1D modulation signalling offers significant power advantages compared to the SC-FDMA with QAM modulations under the same condition of band-limitation. To show the power

reduction gap in between the BER curves of HT-FOFDM and SC-FDMA, we assess the $E_b/N_0$ at BER of $10^{-5}$. When achieving the spectral efficiencies $\eta = 4$, 8 and 12 bits/s/Hz, PAM-M HT-FOFDM has power advantages of 3.5 dB, 9.1 dB and 14.7 dB, respectively, with respect to SC-FDMA with different QAM schemes (($M =$16, 256, 4096).

Moreover, to clearly show the performance advantages of the proposed signalling scheme, we studied the constellation diagrams of the received contaminated HT-FOFDM signals modulated by various PAM schemes and SC-FDMA with the aforementioned QAM schemes. For clarity, the arrangement is held by comparing the constellations between the two schemes of the same spectral efficiencies at certain $E_b/N_0$ values where the performance of HT-FOFDM reaches the BER of $10^{-5}$. Specifically, we conducted the simulations at $E_b/N_0 =$9.8 dB for (a) with (d), 13.4 dB for (b) with (e) and 17.9 dB for (c) with (f) as depicted in Fig. 6 and the associated BER versus $E_b/N_0$ performance of these signals are marked in Fig. 8. The numerical results show the more clear constellations for HT-FOFDM signals with all considered PAM schemes relative to those of SC-FDMA, as expected, indicating that better performance can be achieved for the proposed signals for the same $E_b/N_0$. The main conclusion can be drawn from Fig.6 and Fig. 8 that HT-FOFDM with 1D PAM modulation has enhanced error performance compared to SC-FDMA with the same spectral efficiency or requires less power when achieving the same BER.

## IV. Conclusions

In this work, we devise an energy and spectrally efficient signalling technique for next generation IoT, using bandwidth compressed FOFDM with single dimensional PAM-M scheme and Hilbert filtering pair. We show that the proposed HT-FOFDM signalling increase the transmission rate, by a factor of 12 relative to standard LTE IoT, effectively maintaining reliable transmission up to 2.16 Mbits/s within the narrowband of 180 kHz. The error performance results show that PAM-M HT-FOFDM comprehensively outperforms SC-FDMA that achieves the spectral efficiency with the significant power advantages for the respective spectral efficiencies of 4, 8 and 12 bits/s/Hz.

## References

[1] O. Vermesan, M. EisenHauer, M. Serrano, P. Guillemin, H. Sundmaeker, E. Z. Tragos, J. Valino, B. Copigneaux, M. Presser, A. Aagaard *et al.*, "The next generation internet of things–hyperconnectivity and embedded intelligence at the edge," *Next Generation Internet of Things. Distributed Intelligence at the Edge and Human Machine-to-Machine Cooperation*, 2018.

[2] *Ericsson Mobility Report*, Ericsson, Nov.2021.

[3] "LTE; Evolved Universal Terrestrial Radio Access (E-UTRA)," *Physical Layer Procedures*, vol. Rel. 14, no. 3GPP Standard TS 36.213 v.14.2.0, Apr 2017.

[4] M. Rodrigues and I. Darwazeh, "Fast ofdm: A proposal for doubling the data rate of ofdm schemes," in *Proceedings of the International Conference on Telecommunications*, vol. 3, 2002, pp. 484–487.

[5] T. Xu and I. Darwazeh, "Non-orthogonal waveform scheduling for next generation narrowband iot," in *2018 IEEE Globecom Workshops (GC Wkshps)*. IEEE, 2018, pp. 1–6.

[6] J. Zhao and A. D. Ellis, "A novel optical fast ofdm with reduced channel spacing equal to half of the symbol rate per carrier," in *Optical Fiber Communication Conference*. Optical Society of America, 2010, p. OMR1.

[7] P. A. Haigh, P. Chvojka, Z. Ghassemlooy, S. Zvanovec, and I. Darwazeh, "Non-orthogonal multi-band cap for highly spectrally efficient vlc systems," in *2018 11th International Symposium on Communication Systems, Networks & Digital Signal Processing (CSNDSP)*. IEEE, 2018, pp. 1–6.

[8] T. Xu and I. Darwazeh, "Non-orthogonal narrowband internet of things: A design for saving bandwidth and doubling the number of connected devices," *IEEE Internet of Things Journal*, vol. 5, no. 3, pp. 2120–2129, 2018.

[9] N. H. Nguyen, B. Berscheid, and H. H. Nguyen, "Fast-ofdm with index modulation for nb-iot," *IEEE Communications Letters*, vol. 23, no. 7, pp. 1157–1160, 2019.

[10] X. Liu and I. Darwazeh, "Quadrupling the data rate for narrowband internet of things without modulation upgrade," in *2019 IEEE 89th Vehicular Technology Conference (VTC2019-Spring)*. IEEE, 2019, pp. 1–5.

[11] ——, "Doubling the rate of spectrally efficient fdm systems using hilbert pulse pairs," in *2019 26th International Conference on Telecommunications (ICT)*. IEEE, 2019, pp. 192–196.

[12] F. Xiong, "M-ary amplitude shift keying ofdm system," *IEEE Transactions on Communications*, vol. 51, no. 10, pp. 1638–1642, 2003.

[13] D. Karampatsis, M. Rodrigues, and I. Darwazeh, "Implications of linear phase dispersion on ofdm and fast-ofdm systems," in *London Communications Symposium UCL*, 2002, pp. 117–120.

[14] M. M. Alavi-Sereshki, "Analytic signals and hilbert transforms," Ph.D. dissertation, Texas Tech University, 1972.

[15] P. A. Haigh, P. Chvojka, S. Zvanovec, Z. Ghassemlooy, and I. Darwazeh, "Analysis of nyquist pulse shapes for carrierless amplitude and phase modulation in visible light communications," *Journal of Lightwave Technology*, vol. 36, no. 20, pp. 5023–5029, 2018.

[16] N. C. Beaulieu, C. C. Tan, and M. O. Damen, "A" better than" nyquist pulse," *IEEE Communications Letters*, vol. 5, no. 9, pp. 367–368, 2001.